Am J Physiol Heart Circ Physiol
281: H895–H902, 2001.

Negative wave reflections in pulmonary arteries

ELLEN H. HOLLANDER,[1] JIUN-JR WANG,[1] GARY M. DOBSON,[1]
KIM H. PARKER,[2] AND JOHN V. TYBERG[1]
[1]*Departments of Medicine and Physiology and Biophysics, Cardiovascular Research Group, University of Calgary, Calgary, Alberta, Canada, T2N 4N1; and* [2]*Department of Biological and Medical Systems, Imperial College, London, United Kingdom, SW7 2BX*

Received 24 July 2000; accepted in final form 27 April 2001

Hollander, Ellen H., Jiun-Jr Wang, Gary M. Dobson, Kim H. Parker, and John V. Tyberg. Negative wave reflections in pulmonary arteries. *Am J Physiol Heart Circ Physiol* 281: H895–H902, 2001.—The pulmonary arterial branching pattern suggests that the early systolic forward-going compression wave (FCW) might be reflected as a backward-going expansion wave (BEW). Accordingly, in 11 open-chest anesthetized dogs we measured proximal pulmonary arterial pressure and flow (velocity) and evaluated wave reflection using wave-intensity analysis under low-volume, high-volume, high-volume + 20 cmH_2O positive end-expiratory pressure (PEEP), and hypoxic conditions. We defined the reflection coefficient R as the ratio of the energy of the reflected wave (BEW [−]; backward-going compression wave, BCW [+]) to that of the incident wave (FCW [+]). We found that $R = -0.07 \pm 0.02$ under low-volume conditions, which increased in absolute magnitude to -0.20 ± 0.04 ($P < 0.01$) under high-volume conditions. The addition of PEEP increased R further to -0.26 ± 0.02 ($P < 0.01$). All of these BEWs were reflected from a site ~3 cm downstream. During hypoxia, the BEW was maintained and a BCW appeared ($R = +0.09 \pm 0.03$) from a closed-end site ~9 cm downstream. The normal pulmonary arterial circulation in the open-chest dog is characterized by negative wave reflection tending to facilitate right ventricular ejection; this reflection increases with increasing blood volume and PEEP.

lung; hemodynamics

IN CONTRAST TO THE SYSTEMIC arterial system, which can be described as a single long vessel (the aorta) with side branches, the pulmonary artery (PA) branches immediately and rapidly within a few centimeters of the heart (11, 12, 30). Reflected waves observed in the aorta have generally been of the closed-end type, where the forward-going compression waves responsible for accelerating the blood out of the ventricle are returned as compression waves that oppose the flow of blood from the ventricle (23–25). This is most clearly indicated in the type A waveforms of older patients (21, 23). In the PA, reflected waves have not been so clearly identified, except in the presence of a vasoconstrictor, i.e., serotonin (2, 29). In the control state, it is generally considered that the PA circulation does not create reflections of significant magnitude and, therefore, that it is optimally coupled with the right ventricle (30). However, having assumed that no energy is added to the system (i.e., that the PA vasculature is passive), Attinger (1) concluded that the only possible explanation for all of the harmonics increasing in magnitude is that incident and reflected waves are superimposed.

To characterize wave reflection in the PA system, we used wave-intensity analysis (WIA) (25, 26) a method that can distinguish between forward- and backward-going waves and identify whether they are compression or expansion waves. As recently demonstrated (33) for the coronary arterial circulation, if wave speed can be determined, the respective intensities of simultaneous forward- and backward-going waves can also be calculated.

The overall pattern of waves observed in the PA is similar to that seen in the systemic arteries (Fig. 1). There is a large forward-going compression wave at the start of systole generated by the contraction of the ventricle, a period in midsystole when there is relatively little wave motion, and a complex of waves starting near the end of systole and continuing into early diastole. In this study, we will concentrate on the waves in early systole, primarily because their interpretation is easier. All of the waves from the previous heartbeat have dissipated during diastole and so the initial (forward) compression wave propagates into a nearly quiescent PA. Thus any backward-going waves are almost certainly reflections of this initial wave.

To generate well-defined waves that we could control and manipulate, we introduced a counter-pulsation balloon into the left atrium (LA) that, by direct transmission through the heart, produced in the PA a forward-going compression wave on inflation and a forward-going expansion wave on deflation (15). We analyzed the behavior of the artificially generated waves under a variety of conditions; i.e., low- and high-blood-volume states, hypoxia, and positive end-expiratory pressure (PEEP), to determine their effects on PA wave reflection. Under all of these conditions, we analyzed the waves that were reflected from the PA vasculature to evaluate the hypothesis that there may

Address for reprint requests and other correspondence: J. V. Tyberg, Dept. Medicine and Physiology and Biophysics, Faculty of Medicine, Univ. of Calgary, 3330 Hospital Dr. NW, Calgary, Alberta T2N 4N1, Canada (E-mail: jtyberg@ucalgary.ca).

The costs of publication of this article were defrayed in part by the payment of page charges. The article must therefore be hereby marked "*advertisement*" in accordance with 18 U.S.C. Section 1734 solely to indicate this fact.

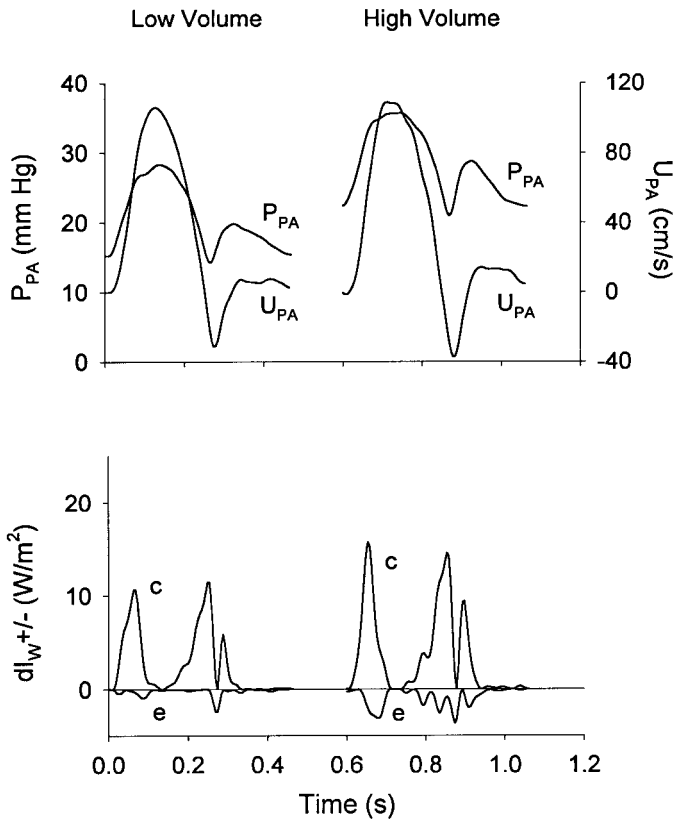

Fig. 1. Proximal pulmonary arterial wave-intensity analysis at low (LoV) and high volume (HiV) and the pressure (P_{PA}) and velocity (U_{PA}) waveforms (*top*) and the corresponding wave-intensity analysis (*bottom*). By convention, intensities of forward-going waves (dI_{W+}) are plotted as positive and intensities of backward-going waves are negative (dI_{W-}); compression waves are denoted by *c* and expansion waves by *e*. Note the forward-going compression wave associated with acceleration of blood out of the ventricle and the backward-going expansion wave that followed. At HiV, note the increased magnitude of the backward-going expansion wave (*e*) relative to the forward-going compression wave (*c*).

be sites in the PA vasculature that have a negative reflection coefficient. It was anticipated that due to its marked and immediate increase in cross-sectional area, the PA circulation might behave in a manner consistent with an open-end reflector, as opposed to the closed-end types of reflections characteristic of the normal systemic circulation.

METHODS

Animal preparation. The studies were performed on 11 dogs (20–27 kg wt) of either gender. Dogs were anesthetized with thiopental sodium (30 μg/kg) and then with 30 $mg \cdot kg^{-1} \cdot h^{-1}$ of fentanyl citrate, and ventilated with a 2:1 NO_2-O_2 mixture using a constant-volume ventilator with a tidal volume of 15 $ml \cdot kg^{-1} \cdot min^{-1}$ (model 607, Harvard Apparatus; Natick, MA). Temperature was maintained at 37°C by a circulating-water warming blanket. A midline sternotomy was performed with the dog in the supine position. The pericardium was opened with an incision along the atrioventricular groove so that the heart could be instrumented. Right and left ventricular pressures (P_{RV} and P_{LV}) were measured using 8-Fr micromanometer-tipped catheters with reference lumens (model PC-480, Millar Instruments; Houston, TX) introduced through a branch of the external jugular vein and carotid artery, respectively. PA and LA pressures (P_{PA} and P_{LA}) were measured with the use of a 3-Fr micromanometer-tipped catheters (model SPR-524, Millar) introduced in a retrograde fashion through small pulmonary arterial and venous branches, respectively. As ascertained by palpation, the PA catheter was advanced within 1 cm of the flowmeter and the LA catheter was advanced just into the LA. Aortic pressure was measured by using an 8-Fr fluid-filled catheter introduced through a femoral artery and was attached to a transducer (model P23ID, Statham-Gould). PA flow was measured using an ultrasonic flowmeter (Transonic Systems; Ithaca, NY) placed on the common PA within 2 cm of the pulmonic valve and converted to velocity (U_{PA}) using a value of cross-sectional area estimated from the size of the flow probe. The time delay in the response of the flowmeter, measured in vitro by comparing the time derivative of the displacement of a syringe pump (measured using a linear potentiometer) to the output of the flowmeter, was 3.5 ± 0.5 ms for the conditions used in the experiments (14, 33). A 35-ml special-order spherical balloon was inserted in to the LA through the appendage and inflated using an aortic counter-pulsation pump (Datascope; Paramus, NJ). The balloon remained deflated until required. The heart was repositioned within the pericardial sac and its margins were loosely reapproximated. A large-bore catheter in the external jugular vein was used to infuse a 2% albumin-saline solution or remove blood for adjustment of the intravascular volume. A single electrocardiographic lead was also recorded. Conditioned signals (model VR16, Electronics for Medicine, Honeywell; Pleasantville, NY) were recorded by a means of a computer using acquisition software (Sonometrics; London, Ontario, Canada). The analog signals were passed through anti-aliasing low-pass filters with a cutoff frequency of 100 Hz and were then sampled at a frequency of 200 Hz. The digitized data were subsequently analyzed with specialized software (CVSOFT, Odessa Computer Systems; Calgary, Alberta, Canada).

The PA micromanometer was referenced to the RV fluid-referenced micromanometer during systole. The LA micromanometer was referenced to the LV fluid-referenced micromanometer during diastole.

Experimental protocol. Of the 11 dogs, the low volume (LoV) and high volume (HiV) protocol and the control balloon inflation protocol were performed in 9 dogs. Of these nine, the PEEP protocol was also performed in six dogs and, of these six, the hypoxia protocol was performed in three dogs. In addition, the hypoxia protocol was performed in two other dogs.

All experimental data were obtained with the ventilator stopped at the end-expiratory position for not more than 20 s. Changes in total blood volume were defined on the basis of changes in LV end-diastolic pressure (P_{LVED}). LoV was defined as P_{LVED} = 4–8 mmHg and HiV was P_{LVED} = 15–20 mmHg. Forward-going PA waves were created by inflation of the LA counter-pulsation balloon under LoV and HiV conditions. With the ventilator turned off, several beats were initially recorded without any intervention (control beats) followed by a rapid, single inflation-deflation of the LA balloon at a specified time during the cardiac cycle (balloon beat). An interval of approximately 100 ms was required to inflate and deflate the balloon. In the proximal PA, inflation generated a forward-going compression wave and deflation, a forward-going expansion wave. Ten to twelve control beats were interposed between balloon inflations. End-expiratory pressure was controlled by putting the end of the gas overflow tube under the surface of the water in a large graduated

cylinder; 20 cm of PEEP was effected by lowering the end of the tube 20 cm under the surface, followed immediately by a single brief flush of oxygen. PEEP data and corresponding control data were obtained under HiV conditions. Hypoxia data and corresponding control data were recorded under LoV conditions. Hypoxia was induced by decreasing the fraction of inspired O_2 and by increasing the fraction of NO_2 delivered by the ventilator. Hypoxia was defined as an arterial P_{O_2} <20 mmHg coupled with an increase in peak systolic P_{PA} of ~10 mmHg.

Data analysis. WIA was used to evaluate the direction, intensity, and type of traveling waves (25). Unlike impedance analysis, which considers the measured pressure and flow waves as the summation of sinusoidal wave trains of different frequencies, this analysis deals with the propagation of infinitesimal wave fronts defined for convenience by the changes in pressure and velocity during each sampling interval. Thus the measured pressure and velocity waveforms are thought of as the summation of successive incremental wave fronts, denoted here simply as "waves." These waves must be considered as pressure-velocity waves because the change in pressure (potential energy) across the wave is related to the change in velocity (kinetic energy).

The direction of the wave was defined in terms of the direction of PA blood flow such that the waves that emanated from the RV were defined as forward going and those from the pulmonary vasculature, backward going. By convention, waves causing an increase in pressure, $dP > 0$ are called "compression" waves and waves causing a decrease in pressure, $dP < 0$ are called "expansion" waves. The intensities (W/m^2) of the forward-going (dI_{W+}) and backward-going waves (dI_{W-}) were calculated from the measured changes in pressure (dP) and velocity (dU) (i.e., the differences between sequential values)

$$dI_{W+} = (dP + \rho c dU)^2/(4\rho c)$$

$$dI_{W-} = -(dP - \rho c dU)^2/(4\rho c)$$

where ρ is the density of blood and c is the wave speed at the point of measurement. Wave speed was calculated as the average value of $dP/\rho dU$ during the ascending phase of pressure and flow in early systole, during which time it was approximately constant and we assumed that no backward-going waves were present (7, 8, 20). These wave speed values were not different from those calculated from characteristic impedance (7, 8, 22).

Forward- and backward-going waves can be either of a compression or expansion type as defined by the signs of dP_+ and dP_-, the respective pressure difference across the forward- and backward-going wave fronts

$$dP_+ = (dP + \rho c dU)/2$$

$$dP_- = (dP - \rho c dU)/2$$

Thus, if dP_+ is >0, the forward-going wave is a compression wave, and, if it is <0, it is an expansion wave. Similarly, if dP_- is greater than zero, the backward-going wave is a compression wave and, if <0, an expansion wave.

The energy (J/m^2) of a forward-going (I_{W+}) or backward-going wave (I_{W-}) was calculated by integrating its intensity (dI_{W+} and dI_{W-}, respectively) over the duration of the wave. For the early-systolic, forward-going compression wave, wave intensity was integrated during the time interval when dP_+ was positive. For the backward-going expansion wave that followed immediately, wave intensity was integrated during the interval when dP_- was negative. For the midsystolic, backward-going compression wave observed under hypoxic conditions, wave intensity was integrated when dP_- was positive.

The magnitude of the reflection was expressed as the reflection coefficient, defined as the ratio of the magnitudes of the energy of the reflected and incident waves, $R = I_{W-}/I_{W+}$. With respect to an initial forward-going compression wave, R was negative if the reflected wave was an expansion wave, as determined by the sign of dP_- at the time of the peak in dI_- ($dP_- < 0$) and positive if it was a compression wave ($dP_- > 0$). This is a departure from previous studies that define the reflection coefficient as the ratio of the pressures of the reflected and incident waves (19). The distance to the site of reflection was estimated by one-half of the time from the peak of the forward-going wave to the peak of the backward-going wave multiplied by the wave speed.

Statistical analysis. Comparisons between beats were made using the analysis of variance with a Bonferroni correction for multiple comparisons; $P < 0.05$ was considered significant. All data are expressed as means ± SE.

RESULTS

The intensities of the forward- and backward-going PA waves are shown on the left side of Fig. 1, indicating that the forward-going compression wave associated with the acceleration of blood out of the RV was followed by a backward-going (reflected) expansion wave. At LoV, the backward-going wave arrived 24 ± 2 ms after the forward-going wave, indicating reflection occurred from a site 3.3 ± 0.5 cm downstream. As the sign of dP_- for the reflected wave was opposite to that of dP_+ for that of the forward-going wave, the wave reflection was negative (i.e., from an open-end type of reflection site); analysis of the ratios of the wave energies indicated that $R = -0.07 \pm 0.02$ (Table 1). Increasing blood volume (HiV) increased R to -0.20 ± 0.04 ($P < 0.01$); it was calculated that the reflected backward-going expansion wave originated from a similar location 2.6 ± 0.3 cm downstream. The increased magnitude of negative reflection with volume loading indicates that the properties of the reflection site have been altered, thus causing a larger proportion of the incident wave to be reflected.

The addition of 20 cmH_2O PEEP at HiV increased R from -0.20 ± 0.03 to -0.26 ± 0.02 ($P < 0.01$, see Fig. 2). Therefore, at HiV, the addition of PEEP increased the magnitude of the open-end type of reflection, thus tending to augment the flow out of the RV somewhat further.

When early-systolic, forward-going, compression waves in the PA were augmented by LA balloon inflation as shown in the right panel of Fig. 3, the energies of the forward- and backward-going waves were increased in proportion, resulting in no significant change in R (Table 1). The character of the reflection from this site is dramatically underscored by the fact that balloon deflation generated a new forward-going expansion wave, which was also reflected negatively as a well-defined backward-going compression wave.

Figure 4 shows one beat recorded under normoxic conditions and one beat recorded under hypoxic conditions. Hypoxia increased peak P_{PA} from 30 ± 3 mmHg to 43 ± 2 mmHg ($P < 0.01$) and increased the slopes of

Table 1. *Wave reflection parameters*

	LoV				HiV			
	Control	Balloon	Normoxia	Hypoxia	Control	Balloon	0 PEEP	20 PEEP
Wave energy, J/m^2								
FCW	0.44 ± 0.06	0.46 ± 0.06	0.42 ± 0.01	1.9 ± 0.5*	0.31 ± 0.05	0.46 ± 0.06†	0.30 ± 0.04	0.31 ± 0.03
BEW	−0.03 ± 0.01	−0.06 ± 0.01	−0.05 ± 0.02	−0.14 ± 0.06	−0.07 ± 0.01	−0.12 ± 0.01†	−0.06 ± 0.01	−0.08 ± 0.02
BCW				0.14 ± 0.03				
Reflection coefficient								
BEW	−0.07 ± 0.02	−0.10 ± 0.02	−0.10 ± 0.05	−0.07 ± 0.02	−0.20 ± 0.04‡	−0.23 ± 0.09	−0.20 ± 0.03	−0.26 ± 0.02†
BCW				0.09 ± 0.03				
Wave speed, m/s	2.8 ± 0.1	3.0 ± 0.3	2.4 ± 0.4	2.3 ± 0.2	2.9 ± 0.3	3.0 ± 0.3	2.9 ± 0.3	2.8 ± 0.6
Distance to reflection site, cm								
BEW	3.3 ± 0.5	2.7 ± 0.4	2.0 ± 0.1	2.1 ± 0.1	2.6 ± 0.3	3.3 ± 0.6	2.7 ± 0.5	2.6 ± 0.5
BCW				9.0 ± 0.1				
n	9	9	5	5	9	9	6	6

Values are means ± SE; *n*, no. of dogs. PEEP, positive end-expiratory pressure. LoV, low volume; HiV, high volume; FCW, forward-going compression wave; BEW, backward-going expansion wave; BCW, backward-going compression wave. *$P < 0.05$; †$P < 0.01$ vs. respective control; ‡$P < 0.01$ vs. LoV control.

both pressure and velocity waveforms (i.e., dP and dU were increased). As evaluated in terms of the early-systolic backward-going expansion wave, negative reflection was maintained in the presence of hypoxia and R was unchanged in magnitude (control, $R = -0.10 \pm 0.05$, and hypoxia, $R = -0.08 \pm 0.03$; $P = 0.6$). In addition; however, the vasoconstricting effect of hypoxia was manifested as a reflected compression wave that arrived in the proximal PA in midsystole, 77 ± 8 ms after the forward-going wave, suggesting a closed-end reflection site 9.0 ± 0.1 cm downstream. This backward-going compression wave increased P_{PA} and decreased U_{PA}, thus tending to impede flow from the RV. The energy of the backward-going compression wave was similar to that of the backward-going expansion wave (Table 1) in that R for the backward-going compression wave was +0.09 ± 0.03. Thus, in the presence of hypoxic conditions, the negative, open-end type reflection was maintained, whereas a positive, closed-end type reflection was created further downstream.

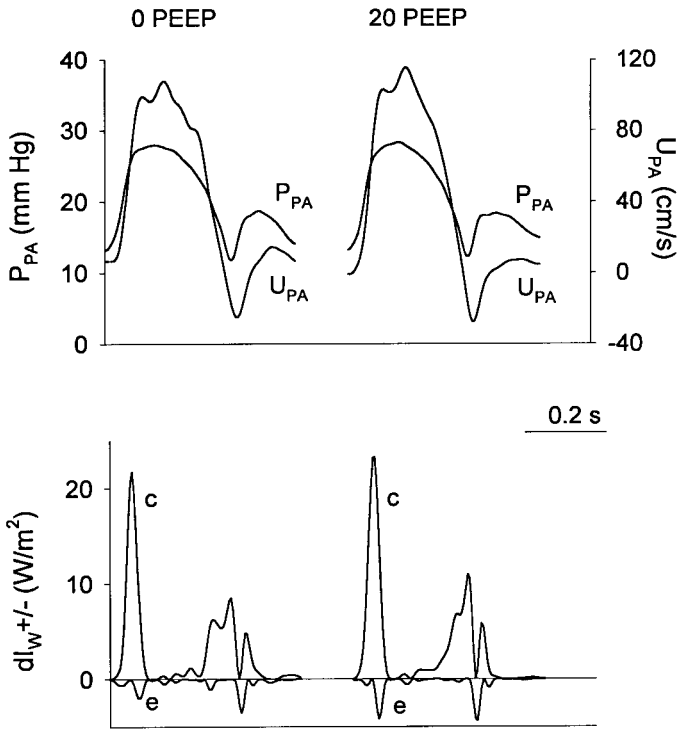

Fig. 2. Proximal pulmonary arterial wave-intensity analysis at 0 and 20 cmH_2O positive end-expiratory pressure (PEEP). Note the larger backward-going expansion wave (*e*) with PEEP (see Fig. 1).

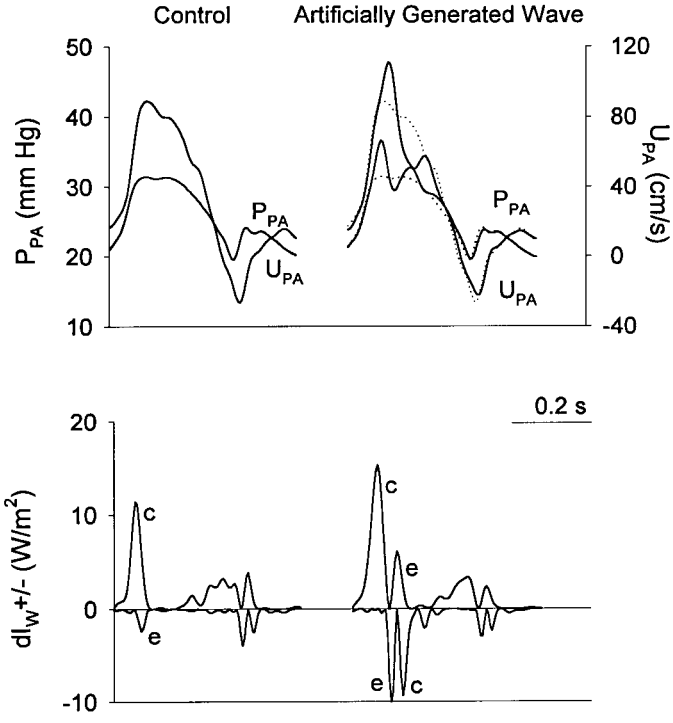

Fig. 3. Proximal pulmonary arterial wave-intensity analysis at HiV showing the effect of an early systolic artificially generated wave. Control conditions (*left*) and effects of early systolic balloon inflation and deflation (*right*). Note that, on balloon deflation, a forward-going expansion wave appeared, which was then reflected as a midsystolic, backward-going compression wave (*bottom right*) (see Fig. 1).

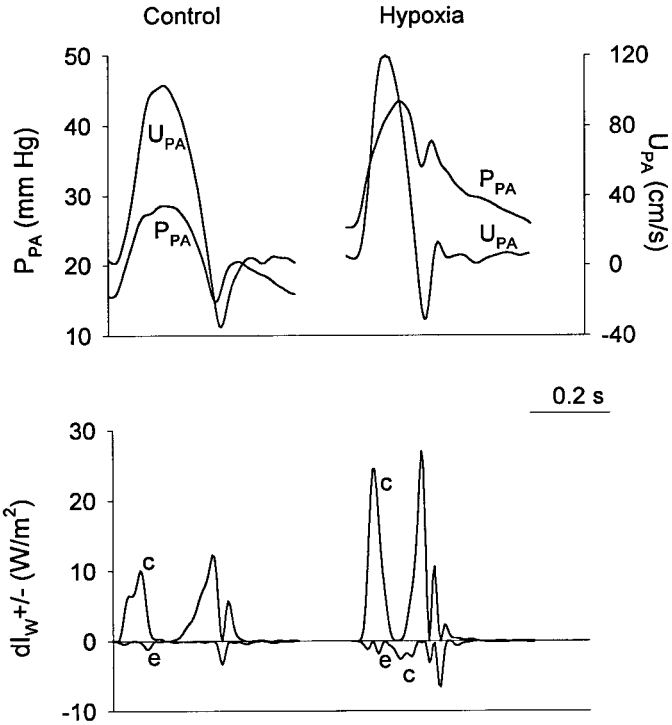

Fig. 4. Proximal pulmonary arterial wave-intensity analysis during hypoxia. Note that there were no changes in the magnitude of the backward-going expansion wave relative to the preceding forward-going compression wave. During hypoxia, there was a backward-going compression wave representing positive wave reflection from constricted arterioles (see Fig. 1).

Because the measured time delay for the flowmeter using the settings employed in these experiments (3.5 ± 0.5 ms) was <1 sampling period, no time shift was used in the calculation of the data presented here. However, because WIA as a time-domain method is particularly sensitive to time delay in the measurements, similar calculations were carried out shifting the velocity measurements relative to the pressure measurements by −5 ms (one sampling period). The resultant changes in the magnitudes of wave intensity and wave energy were minimal and none of the qualitative results of the study were affected by this correction (14).

DISCUSSION

Our major finding is that wave reflections in the proximal PA are negative, indicating that they arise from an open-end type of reflection site located in the proximal portion of the pulmonary arterial tree. The compression wave that is associated with early-systolic acceleration of blood out of the RV was reflected as a backward-going expansion wave, which tended also to accelerate the flow of blood. This backward-going expansion wave has a "pulling" type of action that tends to draw the blood forward, thus supplementing the action of the forward-going compression wave directly generated by the RV. The magnitude of the negative reflection and the further acceleration it provided was augmented by increasing blood volume and by PEEP. Hypoxia, a known pulmonary vasoconstricting stimulus with effects similar to serotonin (2, 29), did not affect the negative reflection site in the proximal portion of the PA (~3 cm from the site of measurement in the main PA), but did create an additional positive reflection site farther downstream (~9 cm from the site of measurement), near the third or fourth generation of arterial branches (1, 27, 29).

These estimates of the locations of the reflection sites are, of course, approximate because their exact determination would require knowledge of the local wave speeds throughout the pulmonary circulation under each experimental condition. Because we can only determine the wave speed in the PA where the pressure and velocity measurements were made, this wave speed was used to estimate the distances of the main reflection sites from the measured delay between the initial FCW and the principal reflections indicated by the peaks in dI_{W-}. As other studies suggest that wave speeds tend to increase peripherally in the pulmonary circulation (1, 27), these estimates probably underestimate the true distances. They do, however, give some indication of the location of the putative reflection sites.

In the pulmonary arterial system, the large increase in cross-sectional area over a short distance (11, 12, 32) is likely to be the primary factor responsible for creating the open-end type of reflections that we measured. The concept of an open-end type of reflection site was described by McDonald (19) and is illustrated in the APPENDIX: "If the termination is closed it will be returned as a positive pressure wave; if the end opens into a large reservoir (an "open" end) it will be returned as a negative wave. This second concept is often found difficult to understand but it is clear that once the fluid flow reaches a reservoir, which is large compared with the volume injected, there will be no pressure variation in that reservoir. The energy of the transmitted wave cannot, by the law of conservation of energy, disappear; thus a wave equal in amplitude but opposite in sign is created."

We have calculated R as the (signed) ratio of the energy of the reflected (backward) wave to that of the incident (forward) wave. Womersley (35) showed that reflection depends on both the area and elastic properties of the vessel such that no reflection will occur if the characteristic impedances on either side of a junction are equal (i.e., the impedances are "matched"). More specifically, with respect to reflection from a given bifurcation, the sign and magnitude of R depend on the characteristic impedances, $Z_n = \rho c_n/A_n$, of the parent and daughter vessels, where A_n and c_n are the area and wave speed of vessel n.

$$R \equiv \frac{I_{W-}}{I_{W+}} = \left[\frac{Z_0^{-1} - (Z_1^{-1} + Z_2^{-1})}{Z_0^{-1} + Z_1^{-1} + Z_2^{-1}}\right]^2$$

where 0 refers to the parent vessel and 1 and 2 refer to the daughter vessels. Because the value of R depends on the areas and wave speeds in the parent and daughter vessels and these parameters will change with

changing experimental conditions, we expect that the value of R for every bifurcation would have changed significantly in the course of our experiments (19, 27). We will therefore discuss our observations in terms of changes in R, the quantity actually measured, and infer the changes in vessel area and distensibility necessary to produce the observed reflections.

For a well-matched symmetrical bifurcation (i.e., a bifurcation at which the characteristic impedances are matched and from which no reflections will emanate), the area ratio of daughter-to-parent areas, $\alpha = (A_1 + A_2)/A_0$, ranges from 1.1 to 1.2, depending on the relationship between area and wave speed for the vessels (19, 20, 22, 28, 34). When α decreases below 1.1, the magnitude of positive, closed-end type reflection will increase; as α increases above 1.2, the magnitude of negative, open-end type reflection will increase. In the PA, values of α from 1.2 to 1.3 have been measured (3, 5, 27). Our observation of negative reflection from a site ~3 cm from the valve implies that α exceeded 1.2 at that site. During hypoxia, our observation of positive reflection from a site ~9 cm from the valve implies that α was <1.1 there.

When we studied the effects of volume loading, the increase in R that we observed (from -0.07 ± 0.02 to -0.20 ± 0.04) suggests that α had increased further at that same reflection site. When intravascular volume was increased, the greater distensibility of the daughter vessels may have led to a greater increase in diameter compared with their parent vessel, and therefore a greater α (9, 11, 18).

When we studied the effects of PEEP, the increase in R that we observed (from -0.20 ± 0.03 [HiV] to -0.26 ± 0.02) suggests that α had increased even further. This increase in the magnitude of R with the addition of PEEP may have been related to a further increase in α caused by a tethering effect of the PEEP-induced expansion of the lung (4, 6, 16, 17). Although PEEP probably increased the diameter of large pulmonary arteries, in our model it may have increased the diameter of the daughter vessels even more. One might expect that PEEP would decrease vessel diameters by compression within the parenchyma of the lung but because we used an open-chest preparation, 20 cmH_2O of PEEP expanded the lungs substantially so that they protruded outward from the cavity and possibly increased vessel diameters. This speculation remains to be confirmed by further studies.

The dramatic increases in R that followed volume loading and PEEP suggest that anything that affects the diameter of the large pulmonary arteries may have substantial implications for wave reflection. The hypoxia data suggest that despite significant vasoconstriction, the negative reflection, which tends to promote flow out of the RV, is maintained, although positive reflection from more distal vessels is also created. The data presented here are compatible with the conclusion that both negative and positive wave reflections are primarily functions of α at given sites, which can be altered independently.

We expressed the energy of the reflected wave as a fraction, R, of the energy of the incident wave. At LoV, the magnitude of the reflected wave was ~8% of the incident wave. Whether this pattern of reflection is "optimal" is not clear. When blood volume was increased (HiV), the magnitude of the backward-going expansion wave increased to ~20% of the incident wave. This would appear to facilitate forward flow substantially, and without any "cost" to the RV. The increased negative reflection with volume loading may have implications in high-cardiac-output states in which RV output can be increased without a proportional increase in RV stroke work. Even though the afterload of the RV is much less than that of the LV, it has seemed remarkable that the thin-walled RV is able to eject the same volume as the LV, an output that may approach 20 l/min in a stressed and trained subject. Negative wave reflection may provide a partial answer to that apparent paradox.

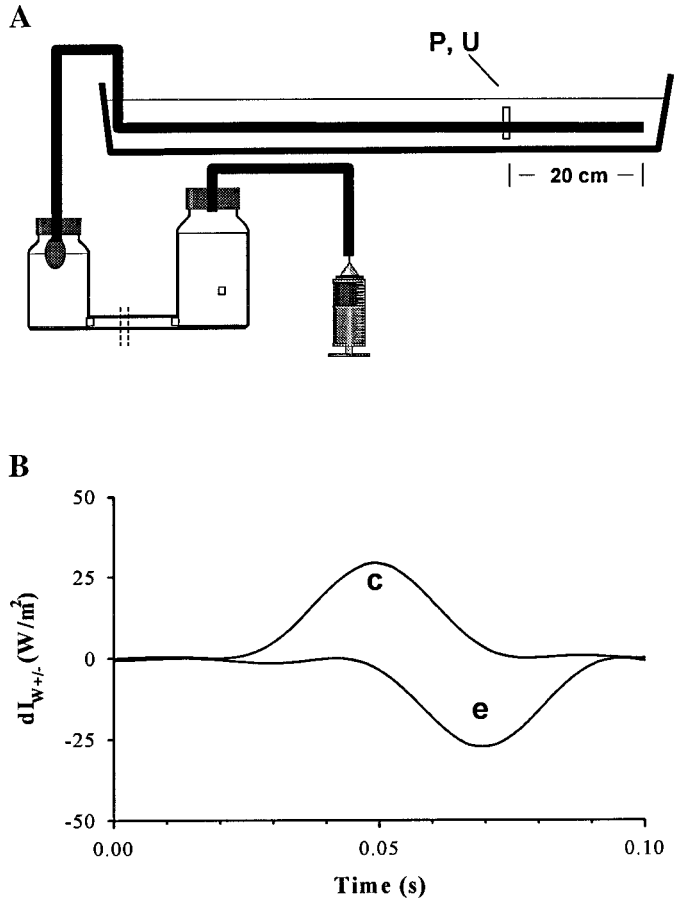

Fig. 5. *Top*: diagram of a bench-top experiment in which a water-containing, flaccid, toy balloon was connected to an open Silastic rubber tube that lay in a water-containing reservoir. The balloon was contained in a bottle, initially open to the atmosphere. By the release of a clamp, the bottle was then connected to a large bottle that had been pressurized to systolic levels. *Bottom*: as observed at a point 20 cm from the open end, an open-end termination reflects a forward-going compression (*c*) wave as a backward-going expansion (*e*) wave. Temporal relation of dI_{W+} and dI_{W-} was similar to that observed in the pulmonary artery (see Fig. 1). Wave speed in the tube was 17 m/s.

The data of Ha et al. (13), who observed a decrease in the backward pressure and an increase in the backward flow waveform early during ejection in chronically instrumented control dogs (see Fig. 6, *top*, of Ref. 13), are compatible with our conclusions. These changes disappeared and evidence for a prominent backward-going compression wave developed in their model of pulmonary hypertension (monocrotaline pyrrole).

For the first time, we have demonstrated an unsuspected feature of the pulmonary circulation that might have very important consequences. However, our experiments were performed in anesthetized open-chest dogs and the magnitude of this negative reflection was not great. Our results are statistically significant but the true significance of our findings cannot be determined until confirmed in people. Fortunately, because WIA only requires simultaneous measurements of pressure and velocity and because high-fidelity measurements of pressure and Doppler measurements of velocity are feasible and convenient in most catheterization laboratories, the results of such clinical studies soon may be forthcoming.

The hemodynamic burden of pulmonary hypertension has never been fully explained by analysis of pulmonary vascular resistance. From these observations, we speculate that pulmonary hypertension might change vascular stiffness or geometry in a way that minimizes or eliminates the negative reflection on which the RV normally depends (10, 31). Alternatively, insofar as clinical pulmonary hypertension resembles the HiV, increased-PA-pressure condition studied here, these patients may already have the benefit of increased negative reflection (although the benefits might be minimized by decreased compliance). In the absence of this "compensating" mechanism, RV ejection might be even further impaired. Clinical studies to test these hypotheses should be undertaken.

In conclusion, by using WIA, we have demonstrated that the normal pulmonary arterial circulation is characterized by negative wave reflections and that the degree of these negative reflections is increased with increasing blood volume and PEEP. This behavior, so fundamentally different from that of the systemic circulation, may help to explain the marked differences between the hemodynamics of the RV and the LV.

APPENDIX

To demonstrate that an open-end reflector (i.e., a reservoir) can transform and reflect a forward-going compression wave into a backward-going expansion wave, we connected a water-contained, flaccid, toy balloon to a long, open, Silastic rubber tube that lay in a reservoir (Fig. 5). Pressure and velocity were measured at several points in the tube. The balloon was contained in a bottle initially open to the atmosphere; then, by the release of a clamp, the bottle was connected to another large bottle that had been pressurized to systolic levels. Thus releasing the clamp was analogous to RV contraction, rapidly raising pressure in the balloon and causing a forward-going compression wave that accelerated the column of water toward the open end of the tube. At the open end, the intensities of the forward-going compression wave and the backward-going expansion wave were symmetrical and approximately equal in magnitude (data not shown). Although the value of R was much higher in the reservoir experiment, at a point 20 cm from the open end (Fig. 5, *bottom*) the temporal relation of the onsets of the two waves was similar to that observed in the PA (see Fig. 1) (wave speed in the tube was 17 m/s). As stated by McDonald and quoted above (19), "an open-end termination causes a positive (i.e., a compression) wave to be reflected as a negative (i.e., expansion) wave."

We acknowledge the excellent technical support provided by Cheryl Meek, Gerald Groves, and Rozsa Sas, the statistical advice of Dr. Rollin Brant of the Centre for the Advancement of Health, and the helpful criticism of Dr. William Whitelaw and Aoife O'Brien. The counter-pulsation balloons were fabricated by Robert Shock and the late Sidney Wolvek of Datascope.

E. H. Hollander held a Studentship from the Heart and Stroke Foundation of Canada (Ottawa). J. V. Tyberg is a Heritage Scientist of the Alberta Heritage Foundation for Medical Research (Edmonton). The study was supported by a Grant-in-Aid from the Heart and Stroke Foundation of Alberta (Calgary) to J. V. Tyberg.

REFERENCES

1. **Attinger EO.** Pressure transmission in pulmonary arteries related to frequency and geometry. *Circ Res* 12: 623–641, 1963.
2. **Bergel DH and Milnor WR.** Pulmonary vascular impedance in the dog. *Circ Res* 16: 401–415, 1965.
3. **Caro CG and Saffman PG.** Extensibility of blood vessels in isolated rabbit lungs. *J Physiol (Lond)* 178: 193–210, 1965.
4. **Cassidy SS and Schwiep F.** Cardiovascular effects of positive end-expiratory pressure. In: *Heart-Lung Interactions in Health and Disease*, edited by Lenfant C. New York: Dekker, 1989, p. 463–485.
5. **Collins R and Maccario JA.** Blood flow in the lungs. *J Biomech* 12: 373–395, 1979.
6. **Culver BH and Butler J.** Mechanical influences on the pulmonary microcirculation. *Annu Rev Physiol* 42: 187–198, 1980.
7. **Dujardin JPL, Stone DN, Forcino CD, Paul LT, and Peiper HP.** Effects of blood volume changes on characteristic impedance of pulmonary artery. *Am J Physiol Heart Circ Physiol* 242: H197–H202, 1982.
8. **Dujardin JP, Stone DN, Paul LT, and Pieper HP.** Response of systemic arterial input impedance to volume expansion and hemorrhage. *Am J Physiol Heart Circ Physiol* 238: H902–H908, 1980.
9. **Engelberg J and DuBois AR.** Mechanics of pulmonary circulation in isolated rabbit lungs. *Am J Physiol* 196: 401–414, 1959.
10. **Fourie PR, Coetzee AR, and Bolliger CT.** Pulmonary artery compliance: its role in right ventricular-arterial coupling. *Cardiovasc Res* 26: 839–844, 1992.
11. **Gan RZ and Yen RT.** Vascular impedance analysis in dog lung with detailed morphometric and elasticity data. *J Appl Physiol* 77: 706–717, 1994.
12. **Glazier JB, Hughes JMB, Maloney JE, and West JB.** Measurements of capillary dimensions and blood volume in rapidly frozen lung. *J Appl Physiol* 26: 65–76, 1969.
13. **Ha B, Lucas CL, Henry GW, Frantz EG, Ferreiro JI, and Wilcox BR.** Effects of chronically elevated pulmonary arterial pressure and flow on right ventricular afterload. *Am J Physiol Heart Circ Physiol* 267: H155–H165, 1994.
14. **Hollander EH.** *Wave-Intensity Analysis of Pulmonary Arterial Blood Flow In Anesthetized Dogs* (PhD thesis). Calgary, Alberta, Canada: University of Calgary, p. 1–140, 1998.
15. **Hollander EH, Parker KH, Gibson DG, and Tyberg JV.** Left atrial pressure perturbations are transmitted to the pulmonary artery more quickly and with less attenuation via the heart than via the pulmonary microcirculation (Abstract). *J Cardiovasc Diag Proc* 13: 295, 1996.
16. **Howell JBL, Permutt S, Proctor DF, and Riley RL.** Effect of inflation of the lung on different parts of pulmonary vascular bed. *J Appl Physiol* 16: 71–76, 1961.

17. **Lieber BB, Li Z, and Grant BJB.** Beat-by-beat changes of viscoelastic and inertial properties of the pulmonary arteries. *J Appl Physiol* 76: 2348–2355, 1994.
18. **Maloney JE, Rooholamini SA, and Wexler L.** Pressure-diameter relations of small blood vessels in isolated dog lung. *Microvasc Res* 2: 1–12, 1970.
19. **McDonald DA.** The relationship between pulsatile pressure and flow. *Blood Flow in Arteries*. London: Arnold, 1974, p. 315–380.
20. **Milnor WR.** *Hemodynamics.* Baltimore, MD: Williams and Wilkins, 1989, p. 42–47.
21. **Murgo JP, Westerhof N, Giolma JP, and Altobelli SA.** Aortic input impedance in normal man: relationship to pressure wave forms. *Circulation* 62: 105–116, 1980.
22. **Nichols WW and O'Rourke MF.** *McDonald's Blood Flow in Arteries*. Philadelphia, PA: Lea and Febiger, 1990, p. 251–267.
23. **Nichols WW, O'Rourke MF, Avolio AP, Yaginuma T, Murgo JP, Pepine CJ, and Conti CR.** Effects of age on ventricular-vascular coupling. *Am J Cardiol* 55: 1179–1184, 1985.
24. **O'Rourke MF.** Pressure and flow waves in systemic arteries and the anatomical design of the arterial system. *J Appl Physiol* 23: 139–149, 1967.
25. **Parker KH and Jones CJH.** Forward and backward running waves in the arteries: analysis using the method of characteristics. *J Biomech Eng* 112: 322–326, 1990.
26. **Parker KH, Jones CJH, Dawson JR, and Gibson DG.** What stops the flow of blood from the heart? *Heart Vessels* 4: 241–245, 1988.
27. **Patel DJ, Schilder DP, and Mallos AJ.** Mechanical properties and dimensions of the major pulmonary arteries. *J Appl Physiol* 15: 92–96, 1960.
28. **Patel DJ and Vaishnav RN.** *Basic Hemodynamics and Its Role in Disease Processes*. Baltimore, MD: University Park Press, 1980.
29. **Piene H.** Influence of vessel distension and myogenic tone on pulmonary arterial input impedance. A study using a computer model of rabbit lung. *Acta Physiol Scand* 98: 54–66, 1976.
30. **Piene H.** Pulmonary arterial impedance and right ventricular function. *Physiol Rev* 66: 606–651, 1986.
31. **Reuben SR.** Compliance of the human pulmonary arterial system in disease. *Circ Res* 24: 40–50, 1971.
32. **Singhal S, Henderson R, Horsfield K, Harding K, and Cumming G.** Morphometry of the human pulmonary arterial tree. *Circ Res* 33: 190–197, 1973.
33. **Sun YH, Anderson TJ, Parker KH, and Tyberg JV.** Wave-intensity analysis: a new approach to coronary dynamics. *J Appl Physiol* 89: 1636–1644, 2000.
34. **Wang JJ.** *Wave Propagation in a Model of the Human Arterial System*. London: Imperial College Press, 1997.
35. **Womersley JR.** Oscillatory flow in arteries: the reflection of the pulse wave at junctions and rigid inserts in the arterial system. *Phys Med Biol* 2: 178–187, 1958.